Time-gated flow cytometry: an ultra-high selectivity method to recover ultra-rare-event μ-targets in high-background biosamples

Dayong Jin
James A. Piper
Macquarie University
Centre of MQ Photonics
New South Wales 2109 Australia

Robert C. Leif
Sean Yang
Newport Instruments
5648 Toyon Road
San Diego, California 92115-1022

Belinda C. Ferrari
University of New South Wales
School of Biotechnology and Biomolecular Sciences
New South Wales 2052 Australia

Jingli Yuan
Guilan Wang
Dalian University of Technology
State Key Laboratory of Fine Chemicals
Dalian 116012, China

Lidia M. Vallarino
John W. Williams
Virginia Commonwealth University
Department of Chemistry
Richmond, Virginia 23284-2006

Abstract. A fundamental problem for rare-event cell analysis is autofluorescence from nontarget particles and cells. Time-gated flow cytometry is based on the temporal-domain discrimination of long-lifetime (>1 μs) luminescence-stained cells and can render invisible all nontarget cell and particles. We aim to further evaluate the technique, focusing on detection of ultra-rare-event 5-μm calibration beads in environmental water dirt samples. Europium-labeled 5-μm calibration beads with improved luminescence homogeneity and reduced aggregation were evaluated using the prototype UV LED excited time-gated luminescence (TGL) flow cytometer (FCM). A BD FACSAria flow cytometer was used to sort accurately a very low number of beads (<100 events), which were then spiked into concentrated samples of environmental water. The use of europium-labeled beads permitted the demonstration of specific detection rates of 100% ± 30% and 91% ± 3% with 10 and 100 target beads, respectively, that were mixed with over one million nontarget autofluorescent background particles. Under the same conditions, a conventional FCM was unable to recover rare-event fluorescein isothiocyanate (FITC) calibration beads. Preliminary results on *Giardia* detection are also reported. We have demonstrated the scientific value of lanthanide-complex biolabels in flow cytometry. This approach may augment the current method that uses multifluorescence-channel flow cytometry gating.
[DOI: 10.1117/1.3103770]

Keywords: flow cytometry; true positive; rare event; europium; time-gated luminescence (TGL); *Giardia*; UV LED; autofluorescence.

Paper 08212R received Jul. 5, 2008; revised manuscript received Nov. 19, 2008; accepted for publication Jan. 27, 2009; published online Apr. 14, 2009. This paper is a revision of a paper presented at the SPIE conference on Imaging, Manipulation, and Analysis of Biomolecules, Cells, and Tissues VI, January 2008, San Jose, California, The paper presented there appears (unrefereed) in SPIE Proceeding Vol. 6859.

1 Introduction

Specific detection of rare-event cells in a rapid and cost-effective fashion remains a challenging issue in biomedicine[1–5] and environmental analysis.[6–8] A rare-event is broadly defined as one that occurs at a frequency of less than 1 in 10,000. Many biological and clinical procedures require accurate detection of rare target cells at frequencies in the range 1 in 1,000,000 or below.[3] For example, residual cancer cells in bone marrow or peripheral blood stem cells preparations used in bone marrow transplantations are a major concern,[9] and it is vital to be able to remove such cells prior to the procedure.[10] This requires a detection level of one residual cancer cell per 10^7 of bone marrow or peripheral blood stem cells. Fetal cells present in maternal blood during pregnancy are an ideal source of genetic material for noninvasive prenatal diagnosis; however, the target fetal nucleated red blood cells (NRBCs) need to be detected against the maternal cells at extremely low frequencies of 1 in 10^7 to 10^9 (Refs. 3, 11, and 12). In water safety inspection, due to the very small number of organisms needed to cause infection, the methods of analysis must be sufficiently sensitive to detect a single microorganism (e.g., *Cryptosporidium parvum* and *Giardia lamblia*) in as many as 10 liters of water containing millions of nontarget microorganisms and particles.[13]

Flow cytometry is the only technique capable of rapidly identifying rare cells from a large sample. It relies on scattering or fluorescence measurements that are made while the cells or particles pass, usually in single file, through a capillary flow cell. Commercial conventional flow cytometry instruments that are equipped with multiple spectral channels are capable of real-time rapid analysis with rates reaching

Address all correspondence to: Dr. D. Jin, Centre of MQ Photonics, Macquarie University, New South Wales 2109 Australia. E-mail: jin@ics.mq.edu.au; and Dr. R.C. Leif, New Port Instruments 5648 Toyon Road, San Diego, CA 92115-1022. E-mail: rleif@rleif.com.

1083-3668/2009/14(2)/024023/10/$25.00 © 2009 SPIE

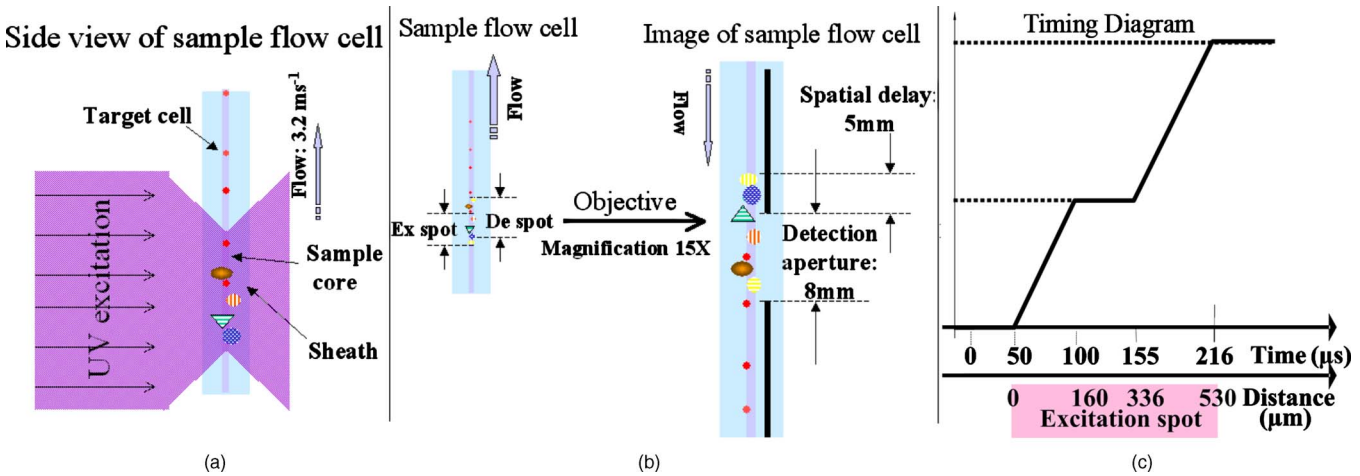

Fig. 1 Schematic geometric layout of TGL FCM. (a) UV LED excitation at flow cell: In the sample flow stream, the solid round (red) particles represent target europium particles/cells, **and** the other larger round (pattern), oval, and triangle particles represent nontarget autofluorescent particles/cells. The smallest illumination spot size from focused UV LED light was 0.53 mm along the flow stream, more than 20 times larger than in conventional flow cytometers that use laser illumination, thus covering many cells instead of a single cell per illumination region. (b). Instead of continuous illumination and detection as in conventional flow cytometers, pulsed excitation and time-gated detection sequence in antiphase are applied to monitor flow sections. This allows both the position and the size of the detection spot to be related to the flow rate and TGL repetition rate in order to discriminate long-lifetime luminescence-labeled cells. The image at the flow cell was magnified (15×) via the signal collection objective optics after projection onto the image plane, which is inverted by the objective. (c) UV exposure compensation in time (upper axis) and distance (lower axis): A cell entering into the excitation spot during the initial UV pulse (100 μs) being less exposed can be compensated by the secondary UV pulse before exiting the UV illumination region. (Color online only.)

100,000 cells/s (Ref. 6). However, detecting such rare events poses significant challenges in terms of accuracy and comes at an unacceptable cost.[10,14] The fundamental challenge is autofluorescence noise from nontarget particle/cells in the complex biological samples.[13,15–17]

We have previously reported a practical flow cytometry method based on the time-gated detection of long-lifetime luminescence-labeled targets.[18,19] The use of time-gated detection of target events in temporal, spectral, and spatial 3-D domains excluded those background particles or cells that otherwise would have been included because their ranges (gates) of light scattering and autofluorescence matched that of the targets. This time-gated detection method enhanced the likelihood of detection of micron-size targets present at a low concentration. This technique showed great potential for the detection of trace amounts of micron-size targets by flow cytometry. However, these studies were limited by the lack of long-luminescent-lifetime calibration beads, which are required for a number of essential experimental activities, such as counting particles, obtaining a histogram of the distribution of particle luminescent intensities, and determining the frequency of rare-event recovery. In this work, a prototype lot of 5-μm europium-labeled beads with long-lived luminescence (~340 μs) was utilized[20] to evaluate the performance of time-gated luminescence (TGL) flow cytometry, with specific focus on the capability of rare-event recovery in environmental samples.

2 Materials and Methods

2.1 *Time-Gated Luminescence Flow Cytometer*

The details of both the concepts and prototype operation of the TGL flow cytometer (FCM) were reported previously.[18,19] Briefly, Fig. 1 shows the basic geometric layout for the current development of the TGL FCM. The targets of interest are labeled with a long-lived luminescent probe, typically a lanthanide complex, and then are excited with a pulsed LED (pulse duration up to 100 μs) as they flow in single-cell profile through the hydrodynamically focused up-flowing laminar stream [Fig. 1(a)]. Once the excitation pulse has extinguished, the autofluorescence fades rapidly (within 0.1 μs). During this time, the luminescence from the targets loses little of its original intensity and continues as the targets progress downstream from the excitation spot. The implementation of periodically pulsed illumination and of time-delayed gated detection has been carefully designed to achieve 100% spatial detection of TGL particles [Fig. 1(b), Table 1], taking into account of the flow speed (3.2 m/s), illumination aperture (530 μm), detection aperture (8 mm), luminescence-label lifetime (340 μs), pulsed illumination (100 μs), and gated-detection-timing sequences.

According to the flow-section model of TGL flow cytometry,[18] the continuous flow stream was conceived as divided into continuously adjacent sections, so that ideally each TGL cycle (consisting of pulsed excitation, time delay, and time-gated detection) can be applied to each section for examining target events within, in order to achieve 100% detection efficiency of sample targets. In this work, a cell takes 166 μs to travel across a UV illumination region of 530 μm (see Table 1); the long pulsed UV-excitation duration (100 μs) resulted in the different position-dependent levels for UV exposure (cells receiving different percentage of pulsed UV exposure) along the flow stream.[18] Fortunately, due to the rapid TGL repetition rate (6.45 kHz), the cells being less exposed from the initial pulse can be compensated by the secondary UV pulse before exiting the UV illumination region, so that the whole flow stream is covered by UV illu-

Table 1 Operational parameters of the TGL flow cytometer.

UV LED pulsed excitation (NCCU033A)	Output wavelength	365 nm
	Current level	1.0 A
	Peak intensity at flow cell	15.0 mW
CPMT gated detection (MH1372)	Quantum yield at 610 nm (europium)	0.09
	Gain	2×10^6
	Preamplifier gain (400-kHz bandwidth)	10^5 V/A
Optics	Excitation filter (SCOTTS UG5 glass)	<400-nm pass
	Dichroic beamsplitter (Zeiss, FT395)	Reflect UV; pass visible
	Emission filter (New Focus, 9514B)	610-nm to 630-nm pass
	Excitation aperture	9 mm diameter
	Condenser lens	40 mm diameter; f=2 mm
	Emission aperture	9 mm long; 1.5 mm wide
	Flow cell objective magnification	×15
	Objective numerical aperture (NA)	1.17 (oil-immersion)
Fluidics: vacuum suction	Flow velocity	3.2 ms^{-1}
	Flow cell dimension	430 μm×180 μm
Timing sequence	TGL cycle rate	6.45 kHz
	Excitation pulse duration	100 μs
	Gate delay time	~10 μs
	Gated detection duration	~40 μs
Geometrical parameters at flow cell	Excitation spot	$(530\ \mu m)^2$
	One excitation profile distance	850 μm
	Flow section distance	496 μm
	Detection region distance	528 μm
	Spatially delayed distance	350 μm
Geometrical parameters at image side	Detection window distance	8 mm
	Detection window delay distance	5 mm
	Image aperture width	1.5 mm

mination without "dead time." Figure 1(c) illustrates such excitation compensation for a cell entering into the excitation spot delayed by 50 μs since switching-on of a UV pulse: for the first 50 μs, the cell was outside the UV illumination spot, and then was illuminated only by the second-half UV pulse for 50 μs after traveling into the excitation spot. During the UV-off period of 55 μs [from 100 μs to 155 μs, upper axis Fig. 1(c)], the cell traveled for 176 μm [from 160 μm to 336 μm, under axis Fig. 1(c)] within the excitation spot. Before exiting the UV excitation region, the second UV pulse will illuminate the cell for another 61 μs [from 155 μs to 216 μs, upper axis Fig. 1(c)]. In total, the cell will accumulate UV exposure for 111 μs. At the TGL repetition rate of 6.45 kHz and flow velocity of 3.2 m/s, all the cells/particles can be excited twice when traveling through the 530 μm UV illumination region. Different position-dependent levels for UV exposure for analytes still exist because luminescence is emitted between the two pulses and cells/particles entering the illumination region at different positions (times in the cycle) receive different proportions of UV from the two pulses.

A new-generation UV LED (maximum CW output power of 250 mW at 365 nm, NCCU033A; Nichia Corp., Japan) generated ~15-mW peak intensity at the flow cell, so the calculated UV excitation efficiency from the full 100-μs pulse was improved[18] from 3.53% to the current 7.56%. At a TGL repetition rate of 6.45 kHz, each flow section covers 496 μm, so the detection region distance is set for 528 μm by detection aperture of 8 mm on the image plane [Fig. 1(b)]. Thus, each TGL section is monitored for 528-μm detection window, within which any time-gated signal pulses with duration of more than 10 μs (filtered by software) can be counted as valid events. In principle, since the particles traveling at flow velocity of 3.2 m/s, the coincidence for the same particle being counted twice in any two adjacent TGL cycles (in the boundary of two adjacent flow sections) is extremely small. In practice, however, a filtering function was programmed in the software to count only events appearing >300 μs away from each other; hence, no long-lifetime luminescent target cells/particles are being counted twice.

Figure 2 shows the optical layout of the UV LED excited TGL FCM. The high-intensity UV LED is mounted on an aluminum plate, which provides improved heat dissipation. The light emitted at a large solid angle (>45 deg) is collected by a high numerical aperture (NA) condenser lens, with the image of the LED projected on the excitation aperture plane, which is positioned directly after a UV excitation filter. The approximately parallel beam is then reflected by the dichroic mirror and redirected into the flow cell objective. Table 1 lists

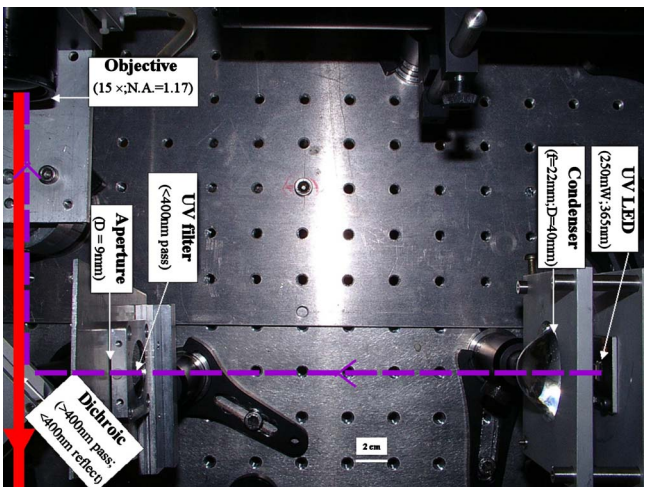

Fig. 2 Layout of the UV LED excitation system that employs epi-illumination optics to excite the TGL FCM. (Color online only.)

the key parameters required for the current version of the TGL FCM to achieve optimum conditions. The TGL repetition rate was 6.45 kHz with excitation pulses of 100 μs, followed by a ~10-μs time-resolving period and a ~45-μs gated-detection period. The average flow velocity was calibrated as to 3.2 m/s (sample flow rate: 100 μL/min). The UV LED was focused to generate a (530-μm)^2 illumination spot with ~15 mW peak power on the sample stream, and the channel photomultiplier tube (CPMT) detector (MH 1372; PerkinElmer Optoelectronics, Germany) operated at a photoelectric gain of $\sim 2 \times 10^6$. The detected anode current from the CPMT was converted to voltage signal by a current-voltage preamplifier (model DHPCA-200, FEMTO, Germany; 400-khz bandwidth; 10^5 V/A). This signal was subsequently digitized by a 1.25-MHz data acquisition card (DAQ; NI PCI-6251, National Instruments Australia Corp., New South Wales, Australia). The memory buffers provided by both DAQ card and personal PC are sufficient for capturing the signal sequence acquired every second, continuously allowing constant real-time data analyzing and presentation in the Labview program. The real-time TGL event counting was programmed with Labview 7.1 Express (National Instruments Australia Corp, New South Wales, Australia).

2.2 *Europium Calibration Beads*

As described in the companion publication,[20] the prototype Newport Instruments Fire Red™ beads were aqueous suspensions of europium-complex-loaded polymer microspheres (beads), which showed low aggregation [see Fig. 3(a) of Ref. 20]. The 5.0-μm europium microspheres had a coefficient of variation (CV) of 7.0% [see Fig. 3(b) of Ref. 20] when measured with a flow cytometer (see Fig. 1 of Ref. 20), which was conventionally gated by wide-angle light-scatter (see Fig. 2 of Ref. 20). The CV of 7.0% establishes that the beads were reasonably uniform in size. The beads contained Eu^{3+} coordination complexes that have an excitation maximum at approximately 370 nm and a very narrow emission near 620 nm, with a luminescence lifetime of 320 ± 30 μs for beads suspended in water (see Fig. 7 of Ref. 20). Before each flow cytometry measurement, the sample was ultrasonicated for 4 min to remove particle aggregation.

2.3 *Flow Cytometric Cell Sorting to Produce Calibration Beads*

Spiked samples of both europium-labeled and FITC-labeled beads, consisting of 10, 100, or 1000 beads, were prepared for recovery determinations. Briefly, calibration spikes were prepared using the BD FACSAria flow cytometer (BD Biosciences, Macquarie Research Park, Sydney, Australia) in single-cell mode. A gate (R1) was defined around the single bead populations within a bivariate dot plot of side scatter scatter (SSC) versus forward scatter (FSC) and events detected in R1 were sorted directly into microfuge or FACS tubes for analysis. Sheath fluid consisted of undiluted Osmosol (Lab Aids Pty. Ltd. Narrabeen, New South Wales, Australia). Each spike calibration set was produced in triplicate for each analysis. Since it is easy to lose subpopulations of cells or particles against the walls of tubes, particularly given the extremely small number (10 or 100) of beads used in this work, the calibration beads were sorted directly into the final test tubes (microfuge tubes were used to contain the europium beads for TGL flow cytometer; FACS tubes were used to contain the FITC-labeled beads for the conventional flow cytometer) or onto the microscopy slides for microscopy confirmation of beads (see the following subsection) without sample transfer steps. In particular, for detection beads from environmental water mud concentrates (Secs. 3.3 and 3.4), the prepared water mud samples (Sec. 2.6) were added into the microfuge tubes or FACS tubes containing the sorted rare-event beads.

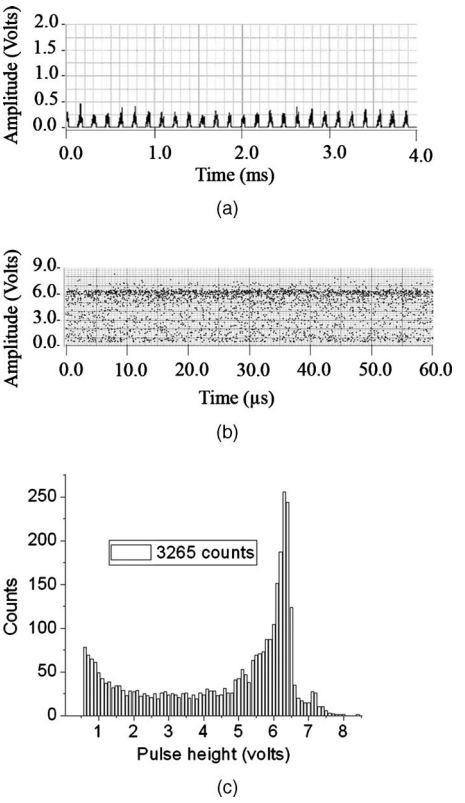

Fig. 3 Real-time counting of europium calibration beads by the UV LED–excited TGL FCM. (a) A 4-ms section of the TGL FCM pulse train during a quiescent period when no particles were present. The minima and maxima of the peaks indicate that the CPMT was in the off and on modes, respectively. The TGL flow-counting background level was less than 0.3 V when there was no TGL event present during the time-gated detection periods. (b) TGL event temporal location. Each cross (+) represents the signal pulse height (V) and arrival time (s) when a TGL event passed the interrogation region of the TGL flow cytometer. (c) Histogram of the signal pulses above 0.5 V. The counts shown on the left below 3 V result from particles that were in the illumination zone during part of the dark period between LED pulses and thus were exposed to UV pulses for less than 100 μs.

2.4 *Microscopy Confirmation of Bead Spikes*

The numbers of beads present in the 100- and 10-bead calibration sets were determined by epifluorescence microscopy using an Axioskop 2 microscope (Carl Zeiss, Sydney, Australia) with appropriate filters for the examination of FITC and europium emissions [4'-6–diamidino-2–phenylindole (DAPI) excitation filter and dichroic mirror]. For the europium-bead preparations, the spike beads sets were 97 ± 1 and 10.3 ± 0.7 for the 100- and 10-bead sample sets, respectively. For the

FITC bead preparations, the spike beads sets were 101 ± 1 and 9 ± 1 for the 100- and 10-bead sample sets, respectively.

2.5 *Giardia Lamblia Cyst Labelling*

As previously reported,[21] an indirect-labeling method was employed to maximize luminescence. Streptavidin (SA) was first conjugated to bovine serum albumin (BSA), and then the SA-BSA conjugate was labeled with a highly luminescent Eu^{3+} complex, 4,4′-bis (1″,1″,1″,2″,2″,3″,3″-heptafluoro-4″, 6*n*-hexanedion-6″-yl)-chlorosulfo-o-terphenyl-Eu^{3+} (BHHCT-Eu^{3+}), to produce the europium complex–labeled SA, $SA(BSA)_{0.9}(BHHCT\text{-}Eu3+)_{46}$. As a result, an average of 46 BHHCT-Eu^{3+} molecules were conjugated to each SA molecule.[21] The original 7-μL solution containing ~1000 *Giardia lamblia* cysts (Biotech Frontiers Pty. Ltd., Sydney, Australia) was incubated for 17 h at room temperature (~20°C) with 10 μL of mouse monoclonal anti-*Giardia* IgG antibody G203 (cyst-wall specific, 40 μg/mL; Biotech Frontiers Pty. Ltd., Sydney, Australia). The sample was then diluted with 300 μL of monoclonal antibody (mAb) buffer, which contains 2 mM tetrasodium pyrophosphate (TSPP); (VWR, http://www.vwrsp.com/); 2% w/v BSA (Sigma-Aldrich), and 0.05% v/v Tween 80 (Sigma-Aldrich); the pH of the buffer was adjusted to ~8.0. The sample was subsequently washed twice with the mAb buffer by centrifugation at 12,000 RPM for 5 min, and the supernatant solution was removed. The sample was then incubated at room temperature for 2 h with 30 μL of a 1:150 dilution of Goat Anti-Mouse Light Chain Specific Biotin Conjugated IgG antibody (Catalogue Number AP200B, Millipore; Chemicon International, Millipore Bioscience Division, Australia). The sample was then washed three times with the mAb buffer. Subsequently, 20 μL of the BHHCT-Eu^{3+}-SA conjugate solution (40 μg/ml) was added and allowed to react for 1 h. This was followed by three washes with 400 μL of the mAb buffer, after which 500 μL of mAb buffer was added to prepare the *Giardia* samples for detection with the TGL FCM. The aim of this work was to evaluate, by the use of a spike-and-recovery method, the current status of the prototype TGL FCM for the detection of microbial cells against an autofluorescent background. No attempt was made to study real-time flow cytometry labeling protocols that would minimize the effect of nonspecific binding to other particles.

2.6 *Environmental Water Sample Preparation*

A large volume of backwash filtered water from a drinking water treatment plant was prepared for use as a quality control sample. Additionally, a 10-L water sample was processed with a calcium carbonate flocculation modified filter to produce a set of 100-mL samples.[22] Following concentration, the water samples were centrifuged for 10 min at 3,500 RPM, and the supernatant was discarded. Prior to use, the concentrates were centrifuged again for 10 min at 13,000 RPM, and the supernatant was discarded. The samples were then resuspended to their initial volume (100 mL) in the mAb buffer and filtered, using a syringe, through a 38-μm stainless steel mesh filter (Metal Mesh Pty., Ltd., Sydney) housed within in a Swinnex filter unit (Millipore, North Ryde, Australia). The samples were forced through the filter to remove large aggregates.

3 Results

3.1 *Real-Time Counting Histogram*

Figure 3(a) shows one typical 4-millisecond section (26 TGL cycles) of the TGL FCM pulse train of a blank sample. It was known from previous work[19] that, under the same operational settings, the real-time observation of signal trains for either pure samples or samples with a large amount of autofluorescence backgrounds showed no difference in terms of background level during the time-gated detection phase. In the experiment illustrated in Figure 3, a sample consisting only of europium calibration beads was tested. Figure 3(a) shows that when no TGL event was present in the time-gated detection periods (corresponding to flow sections that did not contain target beads), the TGL flow counting background level was less than 0.3 V. With the UV LED switched off, only the CPMT dark count (electronic noise) was occasionally observed during the time-gated detection periods (data not shown). When the UV LED injection current was increased, the background level also increased, until it become independent of the LED injection current in the range between 0.2 A and 1 A. As previously noted,[23,24] most of the background detected in the time-gated phase was the result of the UV LED native emissions, which were detected by the CPMT detector in spite of it being shielded by a 610-nm to 640-nm bandpass filter. In order to generate reliable TGL detection data, a pulse detection threshold of 0.5 V was set for all work reported in this paper.

A concentration of approximately 30,000 europium-loaded beads/mL was sufficient to generate statistically valid histogram data. The arrival rate of target beads was calculated from the sample flow rate (~100 μL/min) to be approximately 50 beads/s. According to the concept paper,[18] at this concentration, the coincidence for two particles arriving in the same flow section is calculated as 0.003%. In practice, there were particles aggregating together (see the second histogram peak in Fig. 3(b) of the companion paper, Ref. 20). Figures 3(b) and 3(c) show the real-time counting results for a one-minute period, with 3,265 TGL events counted. Figure 3(b) shows the TGL event temporal locations; each cross (+) marker represents the signal pulse height (*y* axis; volts) and arrival time (*x* axis; μs) when a TGL event passed the detection region of the TGL FCM. Figure 3(c) shows the histogram for the signal pulses above 0.5 V. Thresholding resulted in the clear area at the bottom of Fig. 3(b).

The use of the new europium calibration beads and of the new UV LED excitation (15-mW peak power at the flow cell, compared to 7 mW in the previously reported work[19]) allowed most of the TGL pulses to be clearly resolved from the background level (0.3 V), and the highest TGL signal pulse was 8.2 V, corresponding to a maximum 27 to 1 signal-to-background ratio. In contrast to our previously reported results,[19] the use of new calibration beads provided minimum aggregation after ultrasonication. If the CV is measured on the high amplitude side, which consists of data obtained from particles with a complete exposure to the UV excitation light, this CV falls to approximately 8%. This is in good agreement with the 7% obtained with the light-scatter gated luminescence analysis described in the companion article.[20] These improvements resulted in experimental data that fit more closely to the predicted theoretical concepts.[18] For example,

81% of the TGL target beads registered into higher channels (>2 V) and the peak channel (mode) was located at approximately 6.3 V, with 62% of the events being located in the region between 4.5 and 8.2 V. The different periods of exposure of the beads to the exciting light and the heterogeneity of the beads are the two factors most likely to contribute to the shape of the profile of the TGL flow counting histogram. Concerning the exposure of the beads, the peak population at higher channels (>4.5 V) reflected the number of europium calibration beads that were exposed to maximum UV LED excitation, 100 μs. In turn, the long "tail" toward lower channels was due to the partial excitation of the europium beads by UV LED pulses, which resulted either from some beads entering the excitation region shortly after the 100-μs UV pulse initiation or from some beads exiting the excitation region shortly before the 100-μs UV pulse completion.[18] The heterogeneity of the emissions of the beads could also result from differences in the volume and/or loading of the calibration beads (This was discussed in detail and shown in Fig. 3(b) of the companion article, Ref. 20). Since the histogram figure reported in Fig. 3(b) of the companion article was generated by the scattering-triggered TGL flow cytometer, each particle was illuminated by the same level of UV excitation, thus the histogram figure does not contain the long "tail" toward lower channels, as shown in the histogram Fig. 3(c) generated by the flow-section TGL FCM. This comparison suggests that the different periods of exposure to the exciting light primarily contributed the long "tail" towards lower channels. The fraction of events that were undetected in this work is expected to be reduced by planned improvements in the instrumentation, as described in Sec. 4.

3.2 *Detection Rates for Rare-Event Counting of Beads*

Three samples, each containing ~100 sorted beads, were examined. Figure 4 presents one of the typical results (sample no. 1). Since some target beads could adhere to both the sample tube and to the injection needle of the flow cell, a number of dilution-washing-mixing steps was performed during the rare-event recovery experiments. The original samples of sorted beads were diluted initially into ~800 μL with the mAb buffer, which resulted in most of the beads being detected during the first ~8 min [Fig. 4(a)]. Without pausing and while continuing the counting by the TGL FCM, the sample tube was washed by the addition of 800 μL of mAb buffer and vortex mixing. This was followed by a further wash with 400 μL of water. Counting was terminated 30 min (1800 s) after initiation. Figure 4(b) is a histogram of the 87 events counted. Due to the low number of target beads, the histogram profile was not sufficiently clear to show consistency with the counting result reported in the preceding subsection. However, the peak channel (mode) at about 6.4 V was still quite clearly populated. The visual count obtained by microscopy for the nominal ~100-bead samples was 97±1. The number of beads detected by the TGL FCM in the three nominal ~100-bead samples was 87, 91, and 85 (87.7 average; 3.5% CV), which is 91% ±3% of the number counted by microscopy.

Six samples containing ~10 sorted beads were examined with the TGL FCM. Figure 5 presents one of the typical results (sample no. 3). The original sorted bead samples

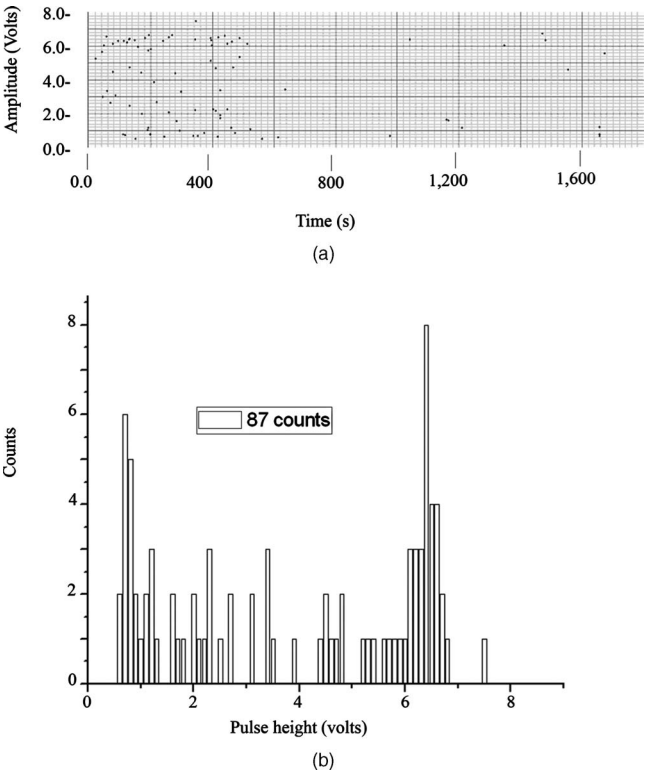

Fig. 4 Detection of the microscopically confirmed 97±1 beads (sample no. 1) with the TGL FCM, resulting in 87 beads counted. (a) Temporal location of TGL events. (b) TGL FCM counting histogram.

(~100 μL) were tested directly without dilution and resulted in the majority of the beads (6 counts for sample nos. 3 and 9 counts in some other samples) being detected in the first ~1 min (data not shown). Without pausing the TGL FCM and while continuing the counting, the sample tube was washed by the addition of ~600 μL of water and vortex mixing; the counting was terminated 8 min after initiation. Figure 5, is a histogram of the 11 events counted. The number of beads detected by the TGL FCM in the six nominal ~10-bead samples was 12, 10, 10, 11, 9, and 11 (10.5 average; 10.0% CV), which is 100% ±20% of the 10±1 counted by microscopy.

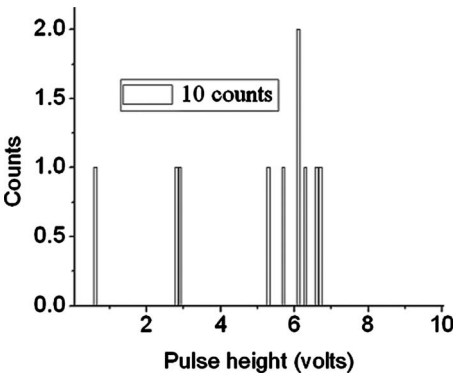

Fig. 5 Detection of the microscopically confirmed 10±1 beads (sample no. 3) with the TGL FCM, resulting in 10 beads counted.

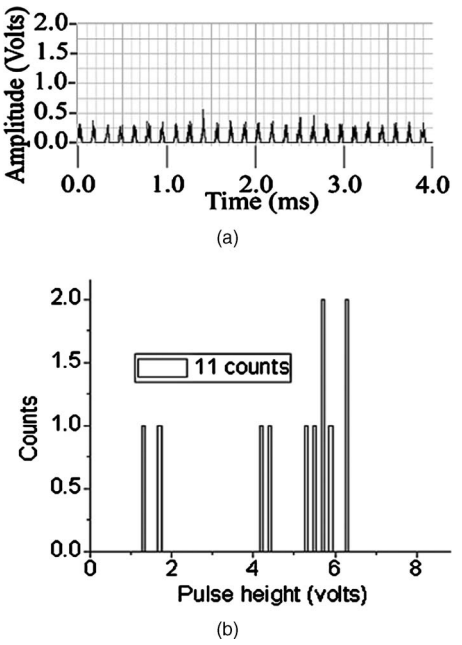

Fig. 6 Detection of the microscopically confirmed 10±1 beads (sample no. 4) from muddy water with the TGL FCM, resulting in 11 beads counted. (a) The TGL flow-counting background level when no TGL event was present in the time-gated detection periods. (b) TGL FCM counting histogram.

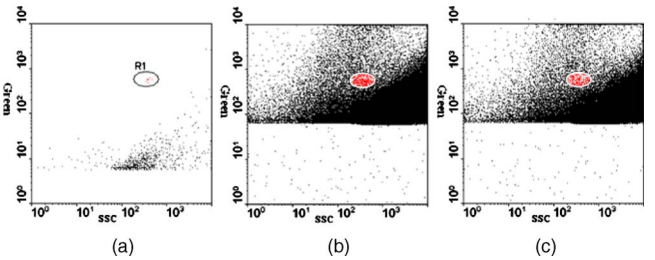

Fig. 7 Detection of FITC beads from muddy water, using a conventional BD FACSCalibur flow cytometer with two-channel regional gating (R1) of the side-scattering (SSC) and green fluorescence (FL1). The counts within the R1 gate are shown in red and outlined in black. (a) Shows that in the case of pure-beads sample counting, very good detection rates (~100%) could be achieved for ~10-bead samples. (b) and (c) Represent two typical results for test samples containing a large number of nontarget particles in muddy water from environmental sources. Region R1 is outlined in white. In these tests, the two-channel-based conventional flow cytometry method lost its discrimination power, as approximately 407 counts and 304 nonspecific counts in the targeted region masked the ~100 and ~10 target FITC beads, respectively, present in the samples. (Color online only.)

3.3 *TGL Detection of Rare-Event Beads from Environmental Water Samples*

Six 10-bead samples were spiked into 200 μL of water-contaminate concentrates (mud) to check the rare-event counting capability offered by the TGL flow cytometry technique with high-background samples. Figure 6(a) shows that the water concentrates did not increase the background level during the time-gated detection phase; Fig. 6(b) presents the histogram of one of the typical results (sample no. 4). Samples that contained both beads and mud background particles (~300 μL) were tested directly without dilution. This resulted in 9 counts in the first ~3 min (event temporal location not shown). Without pausing the TGL FCM and while continuing the counting, the sample tube was then washed by the addition of ~400 μL of water and vortex mixing; counting was terminated 8 min (480 s) after initiation. Figure 6(b) is a histogram of the 11 events counted. The number of beads detected by the TGL FCM in the six nominal ~10-bead samples was 13, 11, 9, 11, 9, and 8 (10.2 average; 18.0% CV), which is 100% ± 30% of that measured by microscopy. There were no counts in the muddy water background samples.

3.4 *Conventional Flow Cytometric Detection of Rare-Event Beads from Environmental Water Samples*

Figure 7 shows a comparison of the recovery data obtained with FITC beads from a pure sample versus a sample in muddy water. These measurements were obtained with a conventional BD FACSCalibur flow cytometer with two-channel regional gating (R1) of the side-scatter (SSC) and green fluorescence. The test procedure was the same as in the TGL FCM evaluations that followed the FACS sorting-microscopic confirmation-spike-flow cytometry evaluation steps. With samples of pure beads, the FACSCalibur detected an acceptable 82% (data not shown) and 100% [Fig. 7(a)] of the 101 ± 1 and 9 ± 1 FITC beads counted by microscopy. However, with environmental samples containing nontarget (background) particles, the two-channel-based conventional flow cytometry technology lost its discrimination power [Figs. 7(b) and 7(c)]. Over 10^6 nontarget autofluorescent particles were detected above the green fluorescence trigger threshold [already increased from 180 units to 450 units, in contrast to the pure bead counting shown in Fig. 7(a)]. The result was 507 and 314 FCM counts in the gated target region (R1) for samples that contained only ~100 beads and ~10 beads, respectively. We demonstrated that FACSCalibur failed to detect rare-event FITC beads in a highly autofluorescence sample, which is a typical example of the challenges encountered in the detection of rapid rare-event microbial cells in environmental samples that contain a large number of nonspecific, intrinsically autofluorescent background cells or particles.

A number of issues need to be addressed here: The detection capability by conventional flow cytometry may be enhanced in the spectral domain by using dual-color coded beads or long Stokes-shift dyes such as PE-Cy5 or PE-Cy7 (or the Alexa analog) or Quantum Dots coded beads (in fact, the best choice would be to use green or red Qdots™ with UV or violet excitation) to avoid greenish autofluorescent backgrounds. Previous research[25] demonstrated the presence of algal cells, which autofluoresce in the red. The presence of photosynthetic organisms is consisted with their findings that FITC excited at 488 nm was the most suitable label for oocysts (detection) in untreated water from 10 liter concentrate, and the fluorochromes CY3, phycoerythin (PE), and tetramethylrhodamine B thioisocyanate (TRITC) excited at 542 nm were the most suitable labels for oocysts in drinking water, where presumably the algal material had been removed. The differences in lifetimes between lanthanide complexes (hundreds of μs) and conventional fluorophores (20 or less nano-

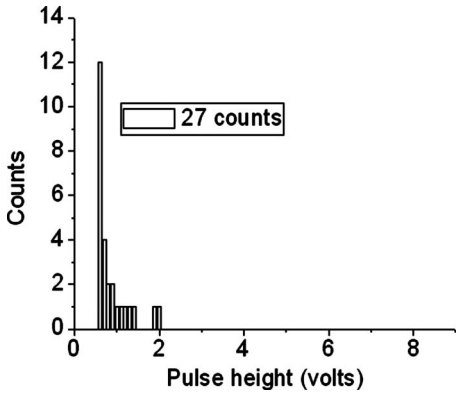

Fig. 8 Preliminary results on the detection of *Giardia* cysts from muddy water using the TGL FCM.

seconds) precluded any reasonable comparison of the two types of labels with the same instrument. At best, only approximately 3% of the europium emission would occur in the detection zone of a conventional flow cytometer. Excitation of the europium-labeled beads would require equipping the FACSCalibur with a 325-nm or 351-nm CW ion laser. Conversely, because of the short lifetime of a quantum dot or a conventional fluorophore, the emissions of these labels would disappear during the ~10 μs time-resolving period before the detector of the TGL FCM becomes fully activated.

3.5 *Giardia Lamblia Cyst Detection by TGL FCM*

The original 100-μL samples containing approximately 200 europium-complex-labeled *Giardia* cysts in muddy water were tested with the current version of the TGL FCM, and 27 events were detected with an approximate detection rate of 13%. (Figure 8 is an example of the preliminary data on *Giardia* cyst detection.) The current prototype failed to detect the majority of the targeted *Giardia* cysts, and all detected events registered into lower channels (<2 volts). The main reason for this result is due to the low excitation efficiency (currently only ~8%) from UV LED; we expect strong excitation from coherent light sources or future development of high power UV LEDs. Second, according to our previous experience with TGL microscopy bio-imaging using europium complex as labels,[24,26] the luminescence intensity of europium complex is increased in aqueous solution by the use of a luminescence enhancement micellular solution.[27,28] Hence, at the next stage of this project, we are going to optimize the europium-labeling protocol including both the antibody-antigen biotin-SA labeling efficiency and the luminescence enhancement buffer for flow cytometry application. However, this result still shows the potential of the TGL flow cytometry technique for use in microbial cell detection, since major improvements in the instrumentation and chemistries can be achieved, as described in the next section.

4 Discussion

Previous reports[1,6,10,16] have demonstrated the challenges encountered by the available flow cytometry technologies for the detection of ultra-rare-events (μ-beads) when a large number of nontarget background particles/cells is also present. In contrast, the new technique for flow cytometry TGL detection reported in this paper has proved successful for the accurate detection of as few as 10 target μ-beads within a population of more than 1,000,000 background particles. In contrast to the conventional multispectrum flow cytometry, the TGL flow cytometry technique here presented a distinctive scenario of extracting temporal (target signal lifetime) fingerprints from target cells. Although in the family of temporal flow cytometry techniques, phase-sensitive flow cytometry[29–34] has been reported, discrimination of individual cells in flow cytometry using the lifetime difference in the nanosecond range could be decreased because of a number of factors that alter the lifetime values, e.g., staining concentration and analysis condition[26] leading to a complex and expensive setup. Lifetime difference permits the detection of the relative amounts of fluorophores with overlapping spectra present. Careful studies on the excitation and emission spectra of a large number of mud samples would be required to determine whether a fluorophore exists that can be sufficiently separated from the autofluorescence of all of the muds to permit background-free detection. The magnitude of the cost of these studies probably is prohibitive. Since time-gated detection of the exceptional long lifetime and large Stokes shift of europium dye probes renders invisible all the background autofluorescence from the particle/cells, ultra-rare-event detection is possible. This has resulted in a practical simple mechanical-optical setup. In conventional flow cytometry, the frequency of target cells per total cells/particles is an essential parameter to calculate rare-cell sampling statistics[27]; while in the flow-section TGL flow cytometry, thanks to the independence of the number of nontarget particles/cells, the frequency of target cells per TGL cycles/sections is the equivalent parameter in order to calculate the rare-cell sampling statistics. For example, when detecting 100 target beads (Sec. 3.2) in 1800 s (30 min) with 11,610,000 decisions (TGL cycles/sections) made, the TGL decision rarity is calculated as one in 116,100, and a theoretical accuracy (assurance) limit can be calculated as ~95% (as described in Ref. 34). Our experimental result of 91% ± 3% closely agrees with the theoretical limit. For the case of 10-bead recovery, the potential error in predicting the correct rare-event frequency gets increasingly larger as the total number of measured rare events becomes very small, as described by Rosenblatt et al.,[27] which also well explained our results of 100% ± 30%. In this work, the development and evaluation of an LED-excited TGL FCM for rare-event counting were based on the availability of low-cost UV LEDs and of new europium-labeled calibration beads, as well as on the sorting capacity of the BD FACSAria flow cytometer, which provided accurate and reliable counts of rare-events in test samples.

The ability of the LED TGL FCM to detect real biological agents can be further increased by improvements in both the instrument design and the detection chemistries. Continued improvements in excitation energy are expected because of the recent, rapid progress in the commercial development of UV LEDs (led by Nichia, Japan), which resulted in both shorter excitation wavelengths and higher peak powers. For example, LEDs with the following properties have been reported recently: 375-nm LED in 2000; 365-nm, 2-mW LED in 2002; 365-nm, 100-mW LED in 2005; and 365-nm,

250-mW in 2007. The cost of UV lasers, such as diode-pumped solid-state (DPSS) Q-switched or diode-based UV lasers, has also decreased sufficiently to make their use commercially feasible.

Improvement in the optics should increase the optical efficiency, which with the currently available UV LED TGL FCM was only ~8% (Ref. 18). The precision of the measurements could be increased significantly by employing an emission detector with a faster turn-on and turn-off, which would permit an increase in the number of excitation-detection cycles. This would lessen the effect of partial illumination of the cells or particles; it would also allow a greater portion of the emitted light to be detected.

Improvements in the detection chemistries will include the use of the europium Quantum Dye, in association with the mononegative anion of thenoyltrifluoroacetone (TTFA) as enhancer.[26,28] This complex has a maximum excitation wavelength that coincides with the emission (365 nm) of the 250-mW UV LED; whereas the optimum excitation wavelength for the europium chelates used in this study is ~336 nm, which does not match the LED emission maximum. The presence of an excess of the $Gd(TTFA)_3$ complex in a micellar solution has been shown to further increase the luminescence of the europium Quantum Dye.[35–37] Polymer carrier technology,[38,39] silica nano-encapsulation technology,[40] and the smaller functionalized beads described in the companion publication[20] could also be applied independently to increase the luminescence.

5 Conclusions

Although lanthanide-complex biolabels have been very popular for spectroscopy, microscopy-type bioassays, and bioimaging, their utility for flow cytometry had been previously questioned by Leif et al.[26,41] It has now been proven that these long-lifetime biolabels can be very useful for rapid cell detection when used with TGL flow cytometry–type instrumentation.

The conventional approach for achieving a highly selective discrimination of target cells in flow cytometry has focused on the use of multicolor biolabels and of multifluorescence-channel gating methods. This work has now demonstrated that rare-event target cells can be discriminated effectively from background by a time-gated method based on long-lifetime luminescent biolabels.

The instrumentation for TGL flow cytometry has the advantage that it allows the use of inexpensive, incoherent solid-state diode sources, thus reducing both the cost and the size of flow cytometers. The success of the tests reported in this paper will lead to further development and applications of the TGL flow cytometer technique in other fields.

Acknowledgments

The authors acknowledge the Australian ARC/NHMRC Fluorescence Applications in Biotechnology and Life Sciences (FABLS) network for a seeding project fund to support emerging new technology, the International Society for Analytical Cytology (ISAC) scholar program, the National Natural Science Foundation of China (No. 20575069), Newport Instruments' Internal Development Funds, and Lidia Vallarino's Gift Fund. Robert C. Leif and Sean Yang are employees of Newport Instruments, which is the supplier of the Fire-Red beads.

References

1. A. D. Donnenberg and V. S. Donnenberg, "Rare-event analysis in flow cytometry," *Clin. Lab Med.* **27**(3), 627-652 (2007).
2. A. L. Allan, S. A. Vantyghem, A. B. Tuck, A. F. Chambers, I. H. Chin-Yee, and M. Keeney, "Detection and quantification of circulating tumor cells in mouse models of human breast cancer using immunomagnetic enrichment and multiparameter flow cytometry," *Cytometry, Part A* **65A**(1), 4–14 (2005).
3. S. Bajaj, J. B. Welsh, R. C. Leif, and J. H. Price, "Ultra-rare-event detection performance of a custom scanning cytometer on a model preparation of fetal nRBCs," *Cytometry* **39**(4), 285–294 (2000).
4. E. A. Jones, A. English, S. E. Kinsey, L. Straszynski, P. Emery, F. Ponchel, and D. McGonagle, "Optimization of a flow cytometry-based protocol for detection and phenotypic characterization of multipotent mesenchymal stromal cells from human bone marrow," *Cytometry, Part B* **70B**(6), 391–399 (2006).
5. K. Yamaguchi, K. Itoh, T. Masuda, A. Umemura, C. Baum, Y. Itoh, T. Okanoue, and J. Fujita, "*In vivo* selection of transduced hematopoietic stem cells and little evidence of their conversion into hepatocytes *in vivo*," *J. Hepatol* **45**(5), 681–687 (2006).
6. B. C. Ferrari and D. Veal, "Analysis-only detection of Giardia by combining immunomagnetic separation and two-color flow cytometry," *Cytometry, Part A* **51A**(2), 79–86 (2003).
7. D. S. Francy, O. D. Simmons, M. W. Ware, E. J. Granger, M. D. Sobsey, and F. W. Schaefer, "Effects of seeding procedures and water quality on recovery of *Cryptosporidium* oocysts from stream water by using US environmental protection agency method 1623," *Appl. Environ. Microbiol.* **70**(7), 4118–4128 (2004).
8. W.-T. Liu and C. Lay, "Lab-on-a-chip devices for microbial monitoring and detection in water," *Water Sci. Technol.: Water Supply* **7**(2), 165–172 (2007).
9. A. B. Deisseroth, Z. F. Zu, D. Claxton, E. G. Hanania, S. Q. Fu, D. Ellerson, L. Goldberg, M. Thomas, K. Janicek, W. F. Anderson, J. Hester, M. Korbling, A. Durett, R. Moen, R. Berenson, S. Heimfeld, J. Hamer, L. Calvert, P. Tibbits, M. Talpaz, H. Kantarjian, R. Champlin, and C. Reading, "Genetic marking shows that Ph(+) cells present in autologous transplants of chronic myelogenous leukemia (Cml) contribute to relapse after autologous bone-marrow in cml," *Blood* **83**(10), 3068–3076 (1994).
10. H. J. Gross, B. Verwer, D. Houck, R. A. Hoffman, and D. Recktenwald, "Model study detecting breast-cancer cells in peripheral-blood mononuclear-cells at frequencies as low as 10(−7)," *Proc. Natl. Acad. Sci. U.S.A.* **92**(2), 537–541 (1995).
11. K. L. Johnson, H. Stroh, K. Khosrotehrani, and D. W. Bianchi, "Spot counting to locate fetal cells in maternal blood and tissue: a comparison of manual and automated microscopy," *Microsc. Res. Tech.* **70**(7), 585–588 (2007).
12. D. W. Bianchi, G. K. Zickwolf, G. J. Weil, S. Sylvester, and M. A. DeMaria, "Male fetal progenitor cells persist in maternal blood for as long as 27 years postpartum," *Proc. Natl. Acad. Sci. U.S.A.* **93**(2), 705–708 (1996).
13. D. A. Veal, D. Deere, B. Ferrari, J. Piper, and P. V. Attfield, "Fluorescence staining and flow cytometry for monitoring microbial cells," *J. Immunol. Methods* **243**(1–2), 191–210 (2000).
14. K. Lemarchand, N. Parthuisot, P. Catala, and P. Lebaron, "Comparative assessment of epifluorescence microscopy, flow cytometry, and solid-phase cytometry used in the enumeration of specific bacteria in water," *Aquat. Microb. Ecol.* **25**(3), 301–309 (2001).
15. H. M. Shapiro, *Practical Flow Cytometry*, 4th ed., John Wiley & Sons, Inc., Hoboken, NJ (2002).
16. B. C. Ferrari, K. Stoner, and P. L. Bergquist, "Applying fluorescence-based technology to the recovery and isolation of *Cryptosporidium* and *Giardia* from industrial wastewater streams," *Water Res.* **40**(3), 541–548 (2006).
17. R. G. McClelland and A. C. Pinder, "Detection of low-levels of specific salmonella species by fluorescent-antibodies and flow-cytometry," *J. Appl. Bacteriol.* **77**(4), 440–447 (1994).
18. D. Jin, R. Connally, and J. Piper, "Practical time-gated luminescence flow cytometry: I. Concepts," *Cytometry, Part A* **71A**(10), 783–796 (2007).

19. D. Jin, R. Connally, and J. Piper, "Practical time-gated luminescence flow cytometry: II. Experimental evaluation using UV LED excitation," *Cytometry, Part A* **71A**(10), 797–808 (2007).
20. R. C. Leif, D. Jin, J. Piper, L. M. Vallarino, J. W. Williams, S. Yang, and R. M. Zucker, "Calibration beads containing luminescent lanthanide ion complexes," *J. Biomed. Opt.* **14**(2), 024022 (2009).
21. J. L. Yuan, G. L. Wang, H. Kimura, and K. Matsumoto, "Highly sensitive time-resolved fluoroimmunoassay of human immunoglobulin E by using a new europium fluorescent chelate as a label," *Anal. Biochem.* **254**(2), 283–287 (1997).
22. G. Vesey, J. S. Slade, M. Byrne, K. Shepherd, and C. R. Fricker, "A new method for the concentration of cryptosporidium oocysts from water," *J. Appl. Bacteriol.* **75**(1), 82–86 (1993).
23. D. Jin, R. Connally, and J. Piper, "Long-lived visible luminescence of UV LEDs and impact on LED excited time-resolved fluorescence applications," *J. Phys. D* **39**(3), 461–465 (2006).
24. R. Connally, D. Y. Jin, and J. Piper, "High intensity solid-state UV source for time-gated luminescence microscopy," *Cytometry, Part A* **69A**(9), 1020–1027 (2006).
25. G. Vesey, D. Deere, M. R. Gauci, K. R. Griffiths, K. L. Williams, and D. A. Veal, "Evaluation of fluorochromes and excitation sources for immunofluorescence in water samples," *Cytometry* **29**(2), 147–154 (1997).
26. R. C. Leif, L. M. Vallarino, M. C. Becker, and S. Yang, "Increasing the luminescence of lanthanide complexes," *Cytometry, Part A* **69A**(8), 767–778 (2006).
27. J. I. Rosenblatt, J. A. Hokanson, S. R. McLaughlin, and J. F. Leary, "Theoretical basis for sampling statistics useful for detecting and isolating rare cells using flow cytometry and cell sorting," *Cytometry* **27**(3), 233–238 (1997).
28. R. C. Leif, L. M. Vallarino, M. C. Becker, and S. Yang, "Increasing lanthanide luminescence by use of the RETEL effect," *Cytometry, Part A* **69A**(8), 940–946 (2006).
29. H. H. Cui, J. G. Valdez, J. A. Steinkamp, and H. A. Crissman, "Fluorescence lifetime-based discrimination and quantification of cellular DNA and RNA with phase-sensitive flow cytometry," *Cytometry, Part A* **52A**(1), 46–55 (2003).
30. C. Deka and J. A. Steinkamp, "Time-resolved fluorescence-decay measurement and analysis on single cells by flow cytometry," *Appl. Opt.* **35**(22), 4481–4489 (1996).
31. B. L. Sailer, J. G. Valdez, J. A. Steinkamp, Z. Darzynkiewicz, and H. A. Crissman, "Monitoring uptake of ellipticine and its fluorescence lifetime in relation to the cell cycle phase by flow cytometry," *Exp. Cell Res.* **236**(1), 259–267 (1997).
32. J. A. Steinkamp and H. A. Crissman, "Resolution of fluorescence signals from cells labeled with fluorochromes having different lifetimes by phase-sensitive flow-cytometry," *Cytometry* **14**(2), 210–216 (1993).
33. J. A. Steinkamp, N. M. Lehnert, J. F. Keij, and B. E. Lehnert, "Enhanced immunofluorescence measurement resolution of surface antigens on highly autofluorescent, glutaraldehyde-fixed cells analyzed by phase-sensitive flow cytometry," *Cytometry* **37**(4), 275–283 (1999).
34. J. A. Steinkamp, B. E. Lehnert, and N. M. Lehnert, "Discrimination of damaged/dead cells by propidium iodide uptake in immunofluorescently labeled populations analyzed by phase-sensitive flow cytometry," *J. Immunol. Methods* **226**(1–2), 59–70 (1999).
35. A. J. Bromm Jr., R. C. Leif, J. R. Quagliano, and L. M. Vallarino, "Addition of a second lanthanide ion to increase the luminescence of europium(III) macrocyclic complexes," *Proc. SPIE* **3604**, 263–272 (1999).
36. R. C. Leif, M. C. Becker, A. J. Bromm Jr., L. M. Vallarino, J. W. Williams, S. A. Williams, and S. Yang, "Optimizing the luminescence of lanthanide(III) macrocyclic complexes for the detection of anti-5BrdU," *Proc. SPIE* **4622**, 250–261 (2002).
37. R. C. Leif, M. C. Becker, A. J. Bromm Jr., L. M. Vallarino, and S. Yang, "Fluorescence resonance energy transfer enhanced luminescence (FRETEL) of Quantum Dyes," *Proc. SPIE* **6092**, 29–41 (2006).
38. R. C. Leif and L. M. Vallarino, "Conjugated polymer tag complexes," International Patent application PCT WO 01/27625, 1–101 (2001).
39. R. C. Leif, M. C. Becker, A. J. Bromm Jr., L. M. Vallarino, S. A. Williams, and S. Yang, "Increasing the luminescence of lanthanide(III) macrocyclic complexes by the use of polymers and lanthanide enhanced luminescence," *Proc. SPIE* **4260**, 184–197 (2001).
40. J. Wu, G. L. Wang, D. Y. Jin, J. L. Yuan, Y. F. Guan, and J. Piper, "Luminescent europium nanoparticles with a wide excitation range from UV to visible light for biolabeling and time-gated luminescence bioimaging," *Chem. Commun. (Cambridge)* **3**, 365–367 (2008).
41. R. C. Leif, S. P. Clay, H. G. Gratzner, H. G. Haines, K. V. Rao, and L. M. Vallarino; "Markers for instrumental evaluation of cells of the female reproductive tract: Existing and new markers," in *The Automation of Uterine Cancer Cytology*, G. L. Wied, G. F. Bahr, and P. H. Bartels, Eds., pp. 313–344, Tutorials of Cytology, Chicago (1976).